

## Aggregation and Chain Dynamics in Supramolecular Polymers by Dynamic Rheology: Cluster Formation and Self-Aggregation

Florian Herbst,<sup>†</sup> Klaus Schröter,<sup>‡</sup> Ilja Gunkel,<sup>‡</sup> Stefan Gröger,<sup>‡</sup> Thomas Thurn-Albrecht,<sup>‡</sup> Jochen Balbach,<sup>‡</sup> and Wolfgang H. Binder<sup>\*†</sup>

<sup>†</sup>*Institute of Chemistry, Division of Technical and Macromolecular Chemistry, Faculty of Natural Sciences II (Chemistry, Physics and Mathematics), Martin-Luther University Halle-Wittenberg, Halle 06120, Germany, and* <sup>‡</sup>*Institute of Physics, Faculty of Natural Sciences II (Chemistry, Physics and Mathematics), Martin-Luther University Halle-Wittenberg, Halle 06120, Germany*

Received August 24, 2010; Revised Manuscript Received October 20, 2010

**ABSTRACT:** Supramolecular polyisobutylenes (PIB) bearing mono- and bifunctional chain ends with hydrogen-bonding units were prepared, and their association behavior in the melt state was investigated by dynamic rheology and compared to aggregation in solution, aiming at determining association dynamics in the solid state. A preparation combining living cationic polymerization with either azide/alkyne “click” reactions or nucleophilic substitution reactions enabled a full end group transformation to the final PIB polymers, modified with either thymine or 2,6-diaminotriazine end groups as proven by NMR and MALDI methods with molecular weights of ~3500 and ~10 000 g/mol. Stoichiometric mixtures of these polymers bearing specifically interacting thymine/triazine moieties were prepared by solution blending and the temperature-dependent dynamics investigated by rheological measurements. At temperatures of 20–60 °C all samples display strongly thermoreversible aggregation with sheet-type or partially cross-linked structures, which deaggregate at temperatures of ~80 °C. More complex aggregates with bridged micellar structure were formed from the respective bifunctional PIB's bearing thymine and 2,6-diaminotriazine moieties. Thus, in addition to specific linear aggregates, the formation of clusters and aggregates of different architecture has to be taken into account to understand and control structure and mechanical properties of supramolecular chains in the melt.

### Introduction

The field of hydrogen-bonded supramolecular polymers is a strongly expanding area, enabling to introduce dynamic features into polymers and polymeric architectures by use of specifically designed noncovalent (supramolecular) interactions. Thus, beside conventional (“covalently-linked”) polymers, hydrogen-bonded polymers have gained in importance over the past two decades,<sup>1–5</sup> most of all with respect to their dynamic properties, generating e.g. self-healing polymers,<sup>6,7</sup> dynamic composites,<sup>8,9</sup> and complex polymeric scaffolds for biomedical applications.<sup>10</sup> In the past years, we have demonstrated the organization of polymeric chains into larger aggregates, such as supramolecular networks<sup>11,12</sup> or highly defined structures such as pseudoblock copolymers.<sup>13,14</sup>

Basically, the dynamics of such materials are determined by two factors: (a) chain dynamics of the individual polymeric building blocks and (b) the inherent dynamics of the connective hydrogen bond, which links the polymeric chains in a defined supramolecular architecture and position.<sup>15</sup> In recent years, significant efforts have been undertaken to achieve a deeper understanding of the inherent dynamics of supramolecular bonds.

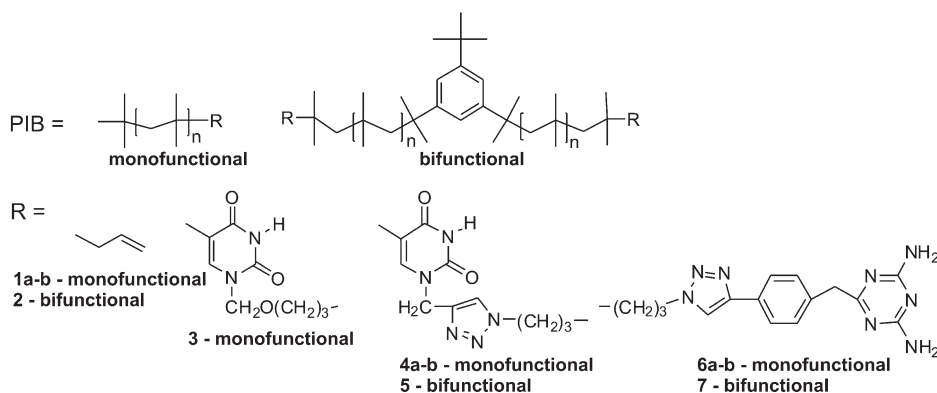
Usually, the dynamics of aggregation in solution has been studied assuming that the basic step of aggregate formation within a simple supramolecular system built from two associating fragments (bearing the respective groups A and B) is diffusion-limited, as described by Hammes et al.<sup>16</sup> The thermodynamic equilibrium constant of association/dissociation in a simple triple hydrogen bond (adenine/uracile) can thus be transformed into the

rate of dissociation, assuming that the associative step is diffusion limited with a constant on the order of  $(1.5–4) \times 10^9 \text{ M}^{-1} \text{ s}^{-1}$ . This concept was then transferred to hydrogen-bonded supramolecular polymers by Meijer et al.,<sup>17</sup> first determining the time scale of opening dynamics of quadruply bound hydrogen bonds (ureidopyrimidine dimers) in solution by spectroscopic techniques. However, it turned out that the purely diffusion-controlled model in this case is not applicable, as tautomeric equilibria change the fraction of molecular collisions between the two associating partners, thus reducing the number of successful dimerization events. Another direct method to probe the supramolecular binding in hydrogen-bonded polymers in solution was achieved by Vancso et al.<sup>18–20</sup> by probing the molecular force between two hydrogen-bonded partners, one affixed onto an AFM tip and the other on a surface, both being connected by transiently associating bifunctional fragments via Meijer's quadrupolar bond. Time-dependent effects of the binding and chain elongation could thus be observed.

Detailed rheological studies of small-molecule associating fragments interconnected by quadrupolar hydrogen bonds (most of all measurements of zero-shear viscosities) by Cohen-Stuart et al.<sup>21,22</sup> subsequently revealed the influence of chain stoppers and temperature on effective chain length and relaxation. Recently, Bouteiller et al. have reported significant clustering of hydrogen bond moieties (bis-ureas) in poly(isobutylene)-modified bis-urea samples<sup>23,24</sup> following early examples of network formation as reported by Stadler et al. in polymeric urazole systems.<sup>25,26</sup> A significant progress has been achieved in gelous network structures, consisting of associating polymers, bound via grafted metal-complexing sites, as discussed by Craig et al.<sup>27–30</sup> These studies allowed an estimation of the dynamics of the underlying supramolecular

\*Corresponding author. E-mail: wolfgang.binder@chemie.uni-halle.de.

**Scheme 1. Chemical Structure and Abbreviations of the Supramolecular Mono- and Bifunctional Polyisobutylenes (PIBs) Bearing Thymine or 2,6-Diaminotriazine Moieties**



bond via frequency-dependent dynamic mechanical measurements of either the viscosity or the storage and loss moduli. Scaling of the respective curves with the known time scale of association in solution led to a superposition of all measured viscosities, thus indirectly allowing the determination of the rates of association.

Studies of chain dynamics in supramolecular polymers in the melt state are rare, as direct measurement techniques and simple models for chain dynamics are not available in dense materials. A recent example was given by Rowan et al.,<sup>31</sup> who described the formation of supramolecular clusters in nucleobase-modified poly(THF) polymers with low molecular weights ( $M_n \sim 1400 \text{ g mol}^{-1}$ ). Multiple stacks were generated by the aromatic moieties of the attached nucleobases. Gel-like network formation was proven by rheological experiments.

The present publication reports on the synthesis and dynamic rheology of mono- or bifunctionalized poly(isobutylenes) PIBs with defined hydrogen-bonding motifs at the chain ends, namely thymine and 2,6-diaminotriazine end group (see Scheme 1). Blends of the different mono- and bifunctional PIBs were investigated. The aim was to study the rheological behavior of the associating system in the bulk and to compare this to the chain dynamics of the unmodified polymer. As PIB can be prepared by living cationic polymerization exact chain length control and low polydispersities are possible. The presented system is highly defined with respect to (a) its molecular weight, (b) its molecular weight distribution, and (c) the number of interacting moieties present at each chain end of the polymer, based on equimolar supramolecular mixtures of the functionalized polyisobutylenes. Poly(isobutylene) was chosen as the central polymer, as it is liquid at room temperature ( $T_g \sim -70^\circ\text{C}$ ) and thus easily allows rheological investigations in bulk without the necessity of added solvents. We find strong effects of supramolecular aggregates on the rheological properties in comparison to the nonfunctionalized PIB. But in general, the formation of supramolecular aggregates in the bulk is more complex than expected from the very selective interactions of the hydrogen-bonding units in solution and is characterized by a variety of structures.

## Experimental Section

**Abbreviations.** Tris[(1-benzyl-1*H*-1,2,3-triazol-4-yl)methyl]amine (TBTA), *N,N*-diisopropylethylamine (DIPEA).

**Materials.** All materials were obtained from Sigma-Aldrich and used without further purification if not mentioned otherwise. Copper iodide triethylphosphite [ $\text{CuI}(\text{P}(\text{OEt})_3)$ ] was synthesized according to Langille et al.<sup>32</sup> 5-Methyl-1-(prop-2-ynyl)-1*H*-pyrimidine-2,4-dione (**8**) was synthesized according to Lindsell et al.<sup>33</sup> Thymine-functionalized PIB (**3**) was synthesized according to Binder et al.<sup>34</sup>

**Synthesis of 6-(4-Ethynylbenzyl)-1,3,5-triazine-2,4-diamine (**9**).** Dicyandiamide (17.70 mmol, 1.49 g), 4-ethynylphenylacetonitrile (4.41 mmol, 600  $\mu\text{L}$ ), and sodium hydroxide (2.21 mmol, 0.14 g) were added to dry isopropanol (60 mL). The mixture was heated under reflux conditions for 24 h, during which the formation of a precipitate was observed. Isopropanol was then decanted, and the residue was heated two times under reflux conditions with isopropanol (70 mL) for 10 min. After drying in high vacuum 919.0 mg (4.08 mmol, 92.5%) of **9** was obtained as a beige solid.  $^1\text{H}$  NMR (400 MHz,  $\text{DMSO}-d_6$ ):  $\delta$  (ppm) 7.39 (d, 2H), 7.27 (d, 2H), 6.62 (s, 4H), 4.10 (s, 1H), 3.65 (s, 2H).  $^{13}\text{C}$  NMR (100 MHz,  $\text{DMSO}-d_6$ ):  $\delta$  (ppm) 175.6, 166.9, 139.9, 131.3, 129.1, 119.4, 83.3, 80.1, 44.2.

**Synthesis of Thymine-Functionalized PIBs via “Click” Reactions (**4**, **5**).** A general procedure for the synthesis of thymine-functionalized PIBs via “click” reactions is shown via the synthesis of monofunctional thymine-functionalized PIB **4b** with  $M_n = 2750 \text{ g/mol}$  (azido-functionalized starting material). In an one-neck round-bottom flask azido-functionalized PIB (0.31 mmol, 852 mg) was dissolved in toluene (17 mL). Water (8 mL), isopropanol (8 mL), compound **8** (0.62 mmol, 102 mg), TBTA (0.03 mmol, 16 mg), and DIPEA (0.62 mmol, 112  $\mu\text{L}$ ) were added. The mixture was sparged with nitrogen for 30 min, bromotris(triphenylphosphine)copper(I) (0.03 mmol, 29 mg) was added, and the flask was sealed with a rubber septum. Subsequently, the flask was placed in the microwave oven and irradiation was started. Microwave conditions were SPS method (“pulse—no pulse—pulse”), reaction temperature  $90^\circ\text{C}$ ,  $\Delta T = 6^\circ\text{C}$ , reaction time 24 h, and an irradiation power of 100 W. After the reaction was finished, the solvent was removed and *n*-hexane was added. The polymer was precipitated into a 10-fold excess of methanol. Pure thymine-functionalized PIB was obtained by column chromatography ( $\text{SiO}_2$ ) in chloroform ( $R_f(\text{4b}) = 0.2$ ). Yield: 708 mg (83%),  $M_n(\text{GPC}) = 3300 \text{ g/mol}$ ,  $M_n(\text{NMR}) = 3200 \text{ g/mol}$ .  $^1\text{H}$  NMR (500 MHz,  $\text{CDCl}_3$ ):  $\delta$  (ppm) 7.80 (s, 1H), 7.37 (s, 1H), 4.97 (s, 2H), 1.91 (s, 5H), 1.44 (bs, 105H), 1.11 (bs, 315H), 0.99 (s, 15H).  $^{13}\text{C}$  NMR (125 MHz,  $\text{CDCl}_3$ ):  $\delta$  (ppm) 163.3, 150.7, 143.8, 140.2, 119.7, 111.2, 59.5, 58.8, 58.2, 55.7, 51.5, 42.8, 42.2, 38.2, 37.8, 37.8, 34.8, 32.6, 32.4, 31.2, 30.8, 30.8, 29.2, 25.5, 12.3.

**Synthesis of 2,6-Diaminotriazine-Functionalized PIBs via “Click” Reactions (**6a**, **b**, **7**).** A general procedure for the synthesis of 2,6-diaminotriazine-functionalized PIBs via “click” reactions is shown via the synthesis of monofunctional 2,6-diaminotriazine-functionalized PIB **6a** with  $M_n = 2600 \text{ g/mol}$  (azido-functionalized starting material). In an one-neck round-bottom flask azido-functionalized PIB (0.93 mmol, 2.42 g) was dissolved in toluene (30 mL). Water (10 mL), isopropanol (10 mL), TBTA (0.19 mmol, 99 mg), and DIPEA (0.14 mmol, 25  $\mu\text{L}$ ) were added. The mixture was sparged with nitrogen for 30 min, copper iodide triethylphosphite (0.09 mmol, 33 mg) and compound **9** (1.12 mmol, 251 mg) were added, and the flask was sealed with a rubber septum.

Subsequently, the flask was placed in the microwave oven and irradiation was started. Microwave conditions were SPS method ("pulse—no pulse—pulse"), reaction temperature 90 °C,  $\Delta T$  6 °C, reaction time 24 h, and irradiation power 50 W. After reaction was finished, the solvent was removed and chloroform was added. The suspension was filtered, and the solvent was removed. Nonfunctionalized polymer chains were separated by column chromatography ( $\text{SiO}_2$ ) in chloroform ( $R_f(\mathbf{6a}) = 0$ ,  $R_f(\text{azido-functionalized PIB}) = 1$ ). After unreacted azido-functionalized PIB was eluted, the solvent mixture was changed to chloroform/methanol = 10/1 and 2,6-diaminotriazine-functionalized PIB was eluted ( $R_f(\mathbf{6a}) = 1$ ). The solvent was removed; the residue was dissolved in a small amount of *n*-hexane and precipitated in a 10-fold excess of methanol. Yield: 1.03 g (43%),  $M_{n(\text{NMR})} = 3960$  g/mol.  $^1\text{H}$  NMR (500 MHz,  $\text{CDCl}_3$ ):  $\delta$  (ppm) 7.78 (d, 2H), 7.71 (s, 1H), 7.39 (d, 2H), 5.31 (bs, 4H), 4.34 (t, 2H), 3.79 (s, 2H), 1.44 (bs, 130H), 1.11 (bs, 390 H), 0.99 (s, 2H).  $^{13}\text{C}$  NMR (125 MHz,  $\text{CDCl}_3$ ):  $\delta$  (ppm) 177.5, 167.0, 147.4, 136.9, 129.6, 129.2, 125.7, 119.2, 59.6, 58.9, 58.3, 55.8, 51.3, 44.8, 42.4, 38.2, 37.9, 37.9, 34.9, 32.7, 32.5, 31.3, 30.9, 30.9, 29.3, 25.7.

**Sample Preparation for Rheological and SAXS Measurements.** Pure PIB samples (**M1**–**M3**, **M5**–**M7**, **M9**–**M11**; see Table 2) were prepared by dissolving the polymer in chloroform. The solution was filtered through a 0.2  $\mu\text{m}$  PTFE filter, and the solvent was removed. The sample was dried in high vacuum to constant weight and annealed at 40 °C for 72 h. For mixtures containing thymine- and 2,6-diaminotriazine-functionalized PIBs (**M4**, **M8**, and **M12**) the amounts needed for an equimolar mixture were calculated from the molecular weight determined via NMR. The amounts were weighed, and the polymers were dissolved in chloroform. After filtration through a 0.2  $\mu\text{m}$  PTFE filter the solutions were combined, and the solvent was removed. Samples were dried in high vacuum to constant weight and annealed at 40 °C for 72 h.

**Methods.** NMR spectra were obtained from a Varian Gemini 2000 (400 MHz) and Varian Unity Inova 500 (500 MHz) spectrometer in  $\text{CDCl}_3$  (liquid NMR). Molecular weights of the PIBs via NMR were determined as follows: For monofunctional PIBs the integral of the initiator at 1.00 ppm was set to 15 H (two overlapping signals with 9 and 6 H). For bifunctional PIBs the integral of the initiator at 7.17 ppm was set to 3 protons.

The resonance of the  $-\text{CH}_2-$  groups of the polymer chain was integrated, and the resulting value was divided by 2 to yield the degree of polymerization (DP). The DP was multiplied by 56.1 g/mol, the molecular weight of the repeat unit, and the molecular weights of the initiator fragment and the introduced end group(s) were added (the end groups conform to the residues "R" in Scheme 1). The added molecular weights of the fragments are (in g/mol) 148.5 for TMPCl (without Cl), 287.3 for DCCl (without Cl), 41 for allyl group, 197.2 for the thymine group introduced via the chloromethyl ether synthesis route, 248.3 for thymine group introduced via the "click" reaction, and 309.4 for the 2,6-diaminotriazine group. Complete functionalization of the monofunctional polymer chains was proven by integrating the signal of the initiator at 1.00 ppm (7.10 ppm for bifunctional PIBs) and setting this value to 15 H (bifunctional: 3 H). The integration of the characteristic resonance of the thymine end group at 7.80 ppm leads to a value of 1 H (bifunctional: 2 H), thus indicating a complete end-group functionalization. The integration of the characteristic resonance of the 2,6-diaminotriazine end group at 3.79 ppm leads to a value of 2 H (bifunctional: 4 H) and indicates a complete functionalization.

**NMR titration experiments** ("Job plots") were performed on a Bruker Avance III spectrometer. The proton frequency was 600.13 MHz, and a BBI probe head was used. Temperature was controlled via a BVT3200 controller. The flip angle was 40°, relaxation delay (RD) was 5 s, and 32 scans were performed for each sample. Temperature calibration was performed using neat methanol and a calibration formula published by Merbach et al.<sup>35</sup> Chemical shifts were recorded in ppm ( $\delta$ ; parts per million)

and referred to the  $-\text{CH}_3$  signal of the PIB chain at 1.10 ppm. The dimerization constant for the 2,6-diaminotriazine group was determined using 2,6-diaminotriazine-functionalized PIB **6a**. The dimerization constant for the thymine group was determined using thymine-functionalized PIB **3**. The association constant for the thymine/2,6-diaminotriazine system was determined by using thymine-functionalized PIB **3** (as host [H]) and 2,6-diaminotriazine-functionalized PIB **6a** (as guest [G]).

**GPC spectra** were recorded on a Viscotek GPCmax VE 2002 solvent/sample module using a  $\text{H}_{\text{HRH}}$  Guard-17369 and  $\text{GM}_{\text{HRH-N-18055}}$  column in THF at 40 °C and a refractive index detector. Polyisobutylene standards were obtained from PSS (Polymer Standards Service) and used for conventional external calibration. Standards with a molecular weight of 340, 1650, 7970, 26 300, 61 800, and 87 600 g/mol were used for calibration.

**MALDI-TOF-MS experiments** were performed on a Bruker Autoflex III system operating in reflectron and linear modes. Ions were formed by laser desorption (smart beam laser at 355, 532, 808, and  $1064 \pm 5$  nm; 3 ns pulse width; up to 2500 Hz repetition rate), accelerated by voltage of 20 kV and detected as positive ions. Baseline subtraction and smoothing of the recorded spectra were performed using a Savitzky–Golay algorithm. The instrument was calibrated with poly(ethylene glycol) (PEG) standards ( $M_n = 2000$  g/mol and  $M_n = 4000$  g/mol) applying a quadratic calibration method with an error of 1–2 ppm. PEG standards (calibration standards) were dissolved in THF at a concentration of 20 mg/mL. *trans*-2-[3-(4-*tert*-Butylphenyl)-2-methyl-2-propenylidene]malononitrile (DCTB) (matrix) and lithium trifluoroacetate (LiTFA) (salt) were dissolved in THF at a concentration of 20 mg/mL. For PEG standards the ratio of matrix:analyte:salt was 100:10:1, and 1  $\mu\text{L}$  of the solution was spotted on a MALDI-target plate. Samples of 2,6-diaminotriazine-functionalized PIBs were prepared by dissolving the polymer in THF at a concentration of 20 mg/mL. Dithranol was used as matrix and dissolved in THF at a concentration of 20 mg/mL. LiTFA was used as salt and dissolved at a concentration of 10 mg/mL. The ratio of matrix: analyte:salt was 100:10:1; the measurement was performed in deflection mode using HPC (high-precision calibration) method. For thymine-functionalized PIBs DCTP was used as matrix.

**Small-angle X-ray scattering experiments (SAXS)** were performed using a Rigaku rotating anode. The X-ray beam was monochromated with an Osmic X-ray optics ( $\lambda = 1.54$  Å). The size of the beam on the sample was  $\sim 300$   $\mu\text{m}$ . Samples were placed in a chamber that was evacuated to a pressure of  $\sim 10^{-1}$  mbar. A Siemens 2D detector with  $1024 \times 1024$  channels was used to count the scattered intensity. Typical measurements took some minutes. Before every measurement the temperature was equilibrated for 15 min.

**Rheological measurements** were performed on an Anton Paar (Physica) MCR 501 using parallel plates (diameter 8 mm). The sample temperature was regulated by thermoelectric cooling/heating in a Peltier chamber under a nitrogen atmosphere. At each temperature the sample was equilibrated for 20 min before the measurement started. All measurements were performed in dynamic mode. After the rheological measurement at 80 °C the measurement at 20 °C was repeated (after temperature equilibration for 30 min). Usually, the results did not differ more than 10% from the first measurement at 20 °C.

## Results and Discussion

**Synthesis of the Polymeric Compounds.** Allyl-functionalized PIBs were synthesized via living carbocationic polymerization as described elsewhere.<sup>36</sup> 2-Chloro-2,4,4-trimethylpentane (TMPCl) was used for the synthesis of monofunctional PIBs, and 1-*tert*-butyl-3,5-bis(1-chloro-1-methylethyl)benzol (DCCl) was used for the synthesis of bifunctional PIBs. The transformation of the allyl-functionalized PIB to the azido-functionalized

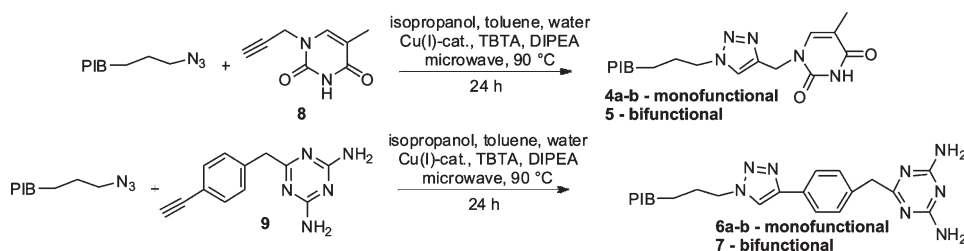


Table 1. Molecular Weight Data of the PIB Building Blocks 1–7

entry	polymer	$M_{n(\text{theor})}$ [g/mol]	$\text{PDI}_{(\text{theor})}^a$	$M_{n(\text{GPC})}^c$ [g/mol]	$M_{n(\text{NMR})}$ [g/mol]	$\text{PDI}^d$	yield <sup>b</sup> [%]
1	<b>1a</b>	3500		3680	3720	1.23	86
2	<b>1b</b>	10000		10600	10900	1.25	93
3	<b>2</b>	3000		2730	2870	1.27	97
4	<b>3</b>	3479	1.20	3500	3600	1.13	75
5	<b>4a</b>	11612	1.24	10900	11400	1.23	73
6	<b>4b</b>	2914	1.23	3300	3200	1.16	83
7	<b>5</b>	3310	1.29	3600	3500	1.34	70
8	<b>6a</b>	2825	1.12	— <sup>c</sup>	3960	— <sup>c</sup>	43
9	<b>6b</b>	7925	1.11	— <sup>c</sup>	7900	— <sup>c</sup>	55
10	<b>7</b>	3625	1.23	— <sup>c</sup>	3700	— <sup>c</sup>	91

<sup>a</sup> PDI of the azido- or hydroxyl-functionalized precursor determined by GPC. <sup>b</sup> Yield of the isolated product. <sup>c</sup> Not possible due to interaction with the GPC column. <sup>d</sup> Determined via GPC. <sup>e</sup> Polyisobutylene standards were used for calibration.

Scheme 2. Synthesis of Mono- and Bifunctional Thymine- and 2,6-Diaminotriazine-Functionalized PIB via the Azide/Alkyne “Click” Reaction



PIB was accomplished according to a method developed by Binder et al.<sup>11,34</sup>

Critical for the following investigations was the synthesis of pure polymeric material, truly containing the hydrogen-bonding end groups (thymine and 2,6-diaminotriazine) affixed to each polymer chain quantitatively. We therefore employed two strategies for the synthesis of the thymine (**3–5**) and triazine (**6, 7**) modified polyisobutylenes, either relying on the previously developed combination of living cationic polymerization with activated chloromethyl ethers (**3**)<sup>34</sup> or via a combination of the living cationic polymerization with azide/alkyne “click” chemistry (**4–7**).<sup>11,37–41</sup> As the first synthetic strategy via chloromethyl ethers is only applicable for monofunctionalized polyisobutylenes up to a molecular weight of  $\sim 10\,000\text{ g mol}^{-1}$ , the “click” approach was probed for the synthesis of bifunctional modified PIBs of medium and higher molecular weights.

Thus, the thymine (**4a,b, 5**) and 2,6-diaminotriazine-functionalized PIBs (**6a,b, 7**) were prepared by azide/alkyne “click” reaction starting from the azido-functionalized PIB species and the corresponding alkyne, bearing the respective supramolecular group (see Scheme 2).

Azido-functionalized PIBs were reacted in a “click”-type reaction with the alkyne-bearing hydrogen-bonding motives **8** and **9** to yield the final 2,6-diaminotriazine (**6a,b, 7**) or thymine functionalized (**4a,b, 5**) PIB polymer, respectively. In all cases, microwave irradiation proved advantageous to achieve a complete conversions of the azide and increases the yield of the final, fully substituted polymer. Both the respective mono- and bifunctionalized polymers (bearing one or two hydrogen-bonding motives at their chain ends) were prepared.

**Characterization of Functionalized PIBs.** Critical for the following rheological investigations was the synthesis of pure polymeric material, truly containing the hydrogen-bonding end groups quantitatively. We therefore confirmed the structure via <sup>1</sup>H and <sup>13</sup>C NMR spectroscopy as well as MALDI-TOF-MS measurements.

Chromatographic and NMR spectroscopic data are shown in Table 1, revealing an excellent match between the  $M_{n(\text{GPC})}$  and  $M_{n(\text{NMR})}$  data, thus indicating a complete end group

functionalization. Because of the strong polarity change after reaction with the thymine as well as the 2,6-diaminotriazine group(s), it was possible to obtain the pure compounds **4–7** after column chromatography, thus removing eventually present impurities or incompletely functionalized polymers. The purity and structure (and complete functionalization in the case of bifunctional PIBs) were confirmed by NMR spectroscopy (Figure 1, see also Supporting Information) and MALDI-TOF-MS analysis (see Figure 1). All compounds showed the expected resonances as well as the expected absolute molecular weights in the respective mass spectra. The MALDI-TOF-MS spectrum for monofunctional thymine-functionalized PIB **4b** is shown in Figure 1b indicating one main series, where each series of ions is separated by 56 Da, the mass of the repeating unit. In agreement with observations made in our group,<sup>34</sup> this signal can be assigned to the expected ion  $[\text{M} \cdot \text{Ag}_2]^+$  assuming exchange of the acidic  $\text{CO}-\text{NH}-\text{CO}$  proton of the thymine group with the  $\text{Ag}^+$  ion of the silver salt. The theoretical  $m/z$  value for the species  $[\text{M} \cdot \text{Ag}_2]^+$  ( $n = 36$ ), 2540.3 Da, is in good agreement with the experimental value of 2541.0 Da. The MALDI-TOF-MS spectra for monofunctional 2,6-diaminotriazine-functionalized PIB **6a** is shown in Figure 1a. The spectrum shows one main series, where again each series of ions was separated by 56 Da, the mass of the isobutylene repeating unit. Signals of the main series can be assigned to the respective  $[\text{M} \cdot \text{H}]^+$  ions of **6a**, while the second minor series can be assigned to  $[\text{M} \cdot \text{Li}]^+$  ions. The theoretical  $m/z$  value for a species  $[\text{M} \cdot \text{H}]^+$  ( $n = 30$ ) is 2050.117 Da, which again is in excellent agreement with the measured value of 2050.592 Da. The same holds true for the theoretical  $m/z$  value for a species  $[\text{M} \cdot \text{Li}]^+$  ( $n = 30$ ) is 2056.126 Da, a value that agrees well with the signal at 2056.598 Da.

**Association in Solution: NMR Titration Experiments.** The thermodynamic association constants in solution were determined via NMR titration experiments using the respective monofunctional polymers. Thus, the association constant ( $K_{\text{assn}}$ ) for the triple hydrogen bond thymine/2,6-diaminotriazine and the corresponding dimerization constants ( $K_{\text{dim}}$ ) were determined using the functionalized PIBs **3** and **6a**. One representative graph is shown in Figure 2 (for more see Supporting Information). The obtained values are in good

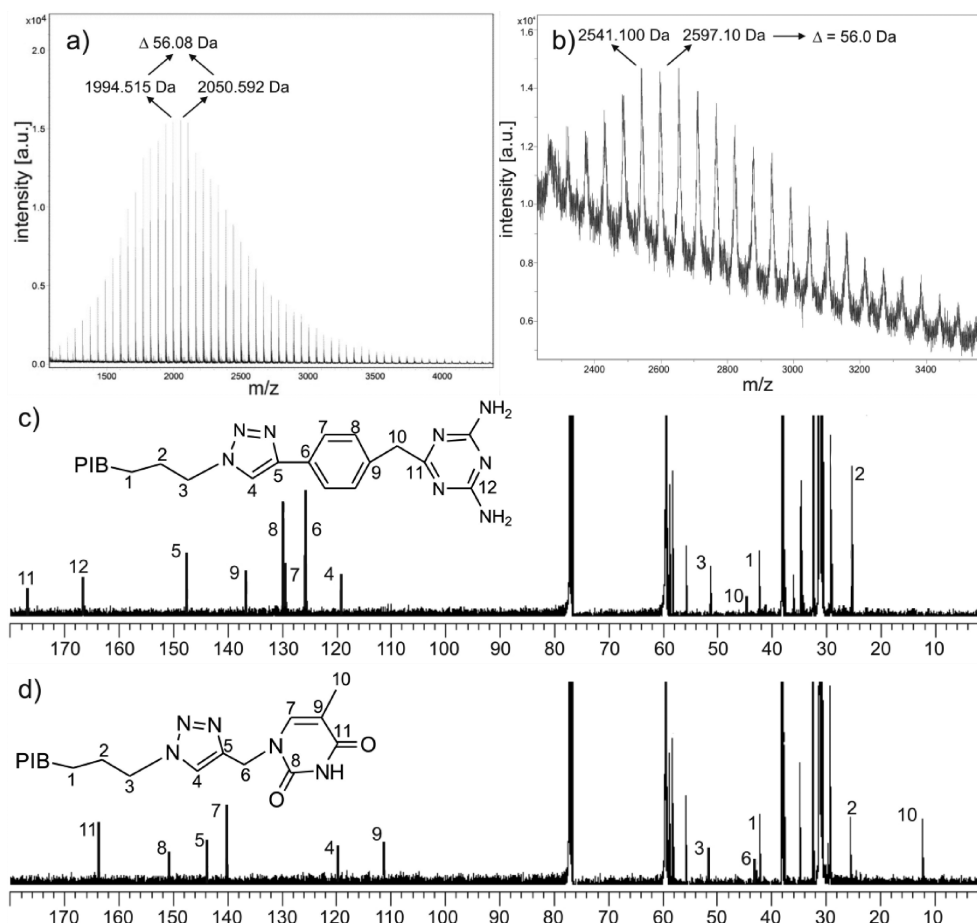


**Figure 1.** (a) MALDI spectrum of 2,4-diaminotriazine-functionalized PIB **6a**, (b) MALDI spectrum of thymine-functionalized PIB **4b**, (c)  $^{13}\text{C}$  NMR spectrum of 2,4-diaminotriazine-functionalized PIB **6a**, and (d)  $^{13}\text{C}$  NMR spectra of the thymine-functionalized PIB **4b**.

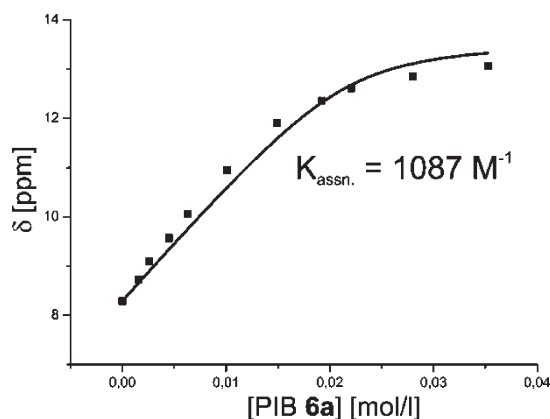


**Figure 2.** NMR titration experiment for the determination of the association constant in solution for the thymine/2,6-diaminotriazine interaction (functionalized PIBs **3** and **6a**). The concentration of PIB **3** was held constant at 0.022 mol/L.

agreement with literature values obtained from low molecular weight compounds. Thus, the association constant ( $K_{\text{assn}}$ ) for the thymine–2,6-diaminotriazine interaction in solution is determined as  $K_{\text{assn}} = 1087 \text{ M}^{-1}$  ( $870 \text{ M}^{-1}$  in the literature<sup>42</sup>), for the thymine/thymine interaction  $K_{\text{dim}}$  as  $3.8 \text{ M}^{-1}$  ( $4.3 \text{ M}^{-1}$  in the literature<sup>42</sup>), and for the triazine/triazine interaction  $K_{\text{dim}}$  as  $1.7 \text{ M}^{-1}$  ( $2.2 \text{ M}^{-1}$  in the literature<sup>42</sup>). The measurements confirmed the much stronger specific interaction of the complementary thymine–triazine groups in solution, compared to the self-aggregation of groups of the

same kind. Accordingly, one would expect also in the melt dominant specific interactions and only to a much lesser extent self-aggregation phenomena.

**Association of Monofunctional Polymers Studied by Melt Rheology.** Any change of molecular weight or architecture of the chain molecules leads to strong changes in the rheological properties. Hence, rheology is well suited to reveal association behavior of PIB equipped with supramolecular entities at its chain ends. Additionally, temperature-dependent measurements give important information on the chain dynamics itself as well as on the temperature-dependent association of the individual polymeric chain ends.

In a first step monofunctional polymers and supramolecular mixtures (consisting of equimolar mixtures of the functionalized polymers with respect to the end group) are investigated by frequency sweep measurements at different temperatures. The supramolecular interaction is based on a triple hydrogen bond, namely the thymine/2,6-diaminotriazine interaction (Figure 3). The possible modes of association in the liquid state for an A/B-type supramolecular polymer are schematically depicted in Figure 3. The desired aggregation between the complementary chain ends A and B as well as self-aggregation between A ends or B ends are possible. On the basis of the association constants from the studies in solution, one would expect an overwhelming contribution of aggregation between the complementary chain ends.

An overview on samples and sample compositions for the rheological measurements is provided in Table 2. Various monofunctional PIBs with molecular weights of  $\sim 3500 \text{ g/mol}$

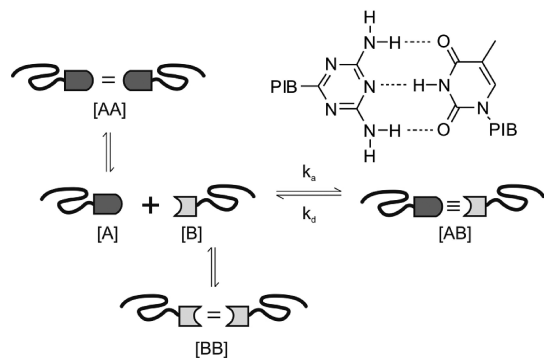


**Figure 3.** Possible modes of association in A/B-type supramolecular polymers in solution. A = thymine groups; B = 2,6-diaminotriazine groups. The inset shows the molecular structure of the hydrogen-bonding groups used.

**Table 2.** Sample Composition and Rheology Data for Homopolymers and Polymer Mixtures M1–M11

entry	name	compound 1	compound 2	$\eta'$ [Pa·s] for $T$ [°C] <sup>a</sup>			
				20	40	60	80
1	M1	1a		299	61	17	6
2	M2	3		1610	201	37	9
3	M3	6a		9980 <sup>b</sup>	2110 <sup>b</sup>	574 <sup>b</sup>	254 <sup>b</sup>
4	M4	6a	3	11800	1420	241	56
5	M5	1b		2430	504	149	65
6	M6	4a		154000 <sup>b</sup>	3300	527	119
7	M7	6b		42 400	7670	1890	407
8	M8	4a	6b	55000	8410	1050	188
9	M9	2		306	59	15	6
10	M10	5		— <sup>c</sup>	— <sup>c</sup>	2370 <sup>b</sup>	292 <sup>b</sup>
11	M11	7		— <sup>c</sup>	— <sup>c</sup>	— <sup>c</sup>	8450
12	M12	5	7	— <sup>c</sup>	— <sup>c</sup>	25000 <sup>b</sup>	1210 <sup>b</sup>

<sup>a</sup> Values for the zero-shear rate viscosity. <sup>b</sup> Sample shows “flowlike” behavior, but terminal flow is not yet reached; i.e., the viscosity is not the true zero shear rate viscosity. Instead, the viscosity at 0.1 s<sup>−1</sup> is displayed.

<sup>c</sup> No flow at this temperature in our frequency range.

(M1–M3) and ~10 000 g/mol (M5–M7) as well as bifunctional PIBs with molecular weights of ~3500 g/mol (M9–M11) were investigated. These are either pure PIBs (allyl-functionalized PIBs) with nonassociative end groups (M1, M5, M9), pure thymine- (M2, M6, M10), or pure 2,6-diaminotriazine-functionalized PIBs (M3, M7, M11). Additionally, exact 1/1 stoichiometric mixtures (with respect to the associative hydrogen-bonding end group) of the thymine-functionalized PIBs and 2,6-diaminotriazine-functionalized PIBs were prepared (M4, M8, M12), enabling the desired A–B-type connection of the PIB chains.

Table 2 also contains the measured zero-shear rate viscosities at 20, 40, 60, and 80 °C. Plots of the viscosity vs temperature are shown in Figure 4a for samples with a molecular weight of ~3500 g mol<sup>−1</sup> and in Figure 4b for samples with ~10 000 g mol<sup>−1</sup>. As anticipated, the viscosity decreases for all polymers and mixtures with increasing temperature as a result of increasing mobility of the polymer chains.

For the series of monofunctional PIBs with a molecular weight of ~3500 g/mol, the nonfunctionalized PIB (M1) shows the lowest viscosity. With the introduction of the thymine moiety (M2) at the PIB chain ends the measurements show an increase of the melt viscosity by a factor of ~5.3 at 20 °C. This can be attributed to the formation of supramolecular aggregates due to the weak interaction between the hydrogen bonds of the thymine moieties.

A similar (self-associative) interaction was also expected for pure 2,6-diaminotriazine-functionalized PIB M3. Figure 4a

reveals a huge increase of the viscosity for sample M3 compared to the nonfunctionalized polymer M1. Additionally, a constant zero shear rate viscosity was not reached (see Figure 5a) although M3 consists of a low molecular weight PIB below the entanglement molecular weight  $M_c$ .<sup>43,44</sup>

Nevertheless, the viscosity at an angular frequency of 0.1 s<sup>−1</sup> is displayed in Table 2 to allow a rough estimate for the viscosity increase, which is higher by a factor of ~33 for M3 in comparison to M1.

Although the dimerization constant of the 2,6-diaminotriazine group in the solution (as determined by NMR titration experiments, vide supra) ( $K_{\text{dim}} = 1.7 \text{ M}^{-1}$ ) is comparable to that of the thymine group ( $K_{\text{dim}} = 3.8 \text{ M}^{-1}$ ), the viscosity increase in the melt is significantly higher in M3 by a factor of ~6 compared to M2, implying a stronger association or larger aggregation number of the polymers bearing the 2,6-diaminotriazine groups in the melt state. As it is well known that melamine and melamine-based system (like the 2,6-diaminotriazine end group of 6b in M3) undergo a strong aggregation in the solid state,<sup>45</sup> we assume a similar aggregation into larger clusters in the case of the polymers containing thymine moieties, as in sample M2 (cf. also SAXS measurements below). Possible structures are shown in Scheme 3a (for M2) as well as the formation of clusters for M3 (Scheme 3b). The observed increase of the viscosity and the fact that no terminal flow is observed (Figure 5a) can thus clearly be assigned to the formation of strong, larger aggregates formed due to the presence of the 2,6-diaminotriazine groups. Similar aggregated structures have been observed before in multifunctional network-forming supramolecular polymers containing uradiazole cross-linkers<sup>46</sup> or urea-based hydrogen bonds.<sup>47</sup>

To what extent self-aggregation is still present in case of the specifically assembling polymer was measured using the pseudo-homopolymer mixture M4. For the equimolar mixture of thymine- and 2,6-diaminotriazine-functionalized PIB M4 the viscosity in comparison to M1 is increased by a factor of ~39.5 (at 20 °C). Although the viscosity values for M4 at lower temperatures are very similar to those of M3, there are significant differences. M4 shows a Newtonian behavior at low frequencies (see Figure 5b). Since M4 is an equimolar mixture of PIB 6a and 3 (and thus an equimolar mixture of thymine and 2,6-diaminotriazine groups), each functional group is able to undergo the supramolecular interaction with its counterpart. This specific interaction is strong and expected to suppress the formation of any other aggregates (e.g., melamine-based cluster). This fact obviously limits the aggregation number or size of the self-aggregates and hence also their effect on viscosity. Accordingly, the zero shear rate viscosity of M4 stays below the (extrapolated) value for M3 (compare parts a and b of Figure 5). But also for M4 more than two chains are found to aggregate. Otherwise, the viscosity increase by a factor of 39.5 compared to M1 could not be understood. For a linear unentangled polymer one would only expect an increase by a factor of 2 for a 2-fold increase in molecular weight by combining two chains at one end. However, as demonstrated by Flory et al.,<sup>44</sup> a nonlinear increase of viscosity was observed at molecular weights (PIB) below 17 000 g mol<sup>−1</sup>. Therefore, the present increase is also partially explained via this unnormal behavior.

The comparable temperature dependence in the viscosity of M3 and the nonfunctionalized polymer M1 shows that the aggregates in M3 are stable over the studied temperature range. The temperature dependence is governed by the chain dynamics. Contrarily, for M4 the viscosity decreases with increasing temperature stronger than for the nonfunctionalized polymer M1. Hence, the dynamics of the supramolecular interaction gain in importance. The associating hydrogen bonds are able to undergo

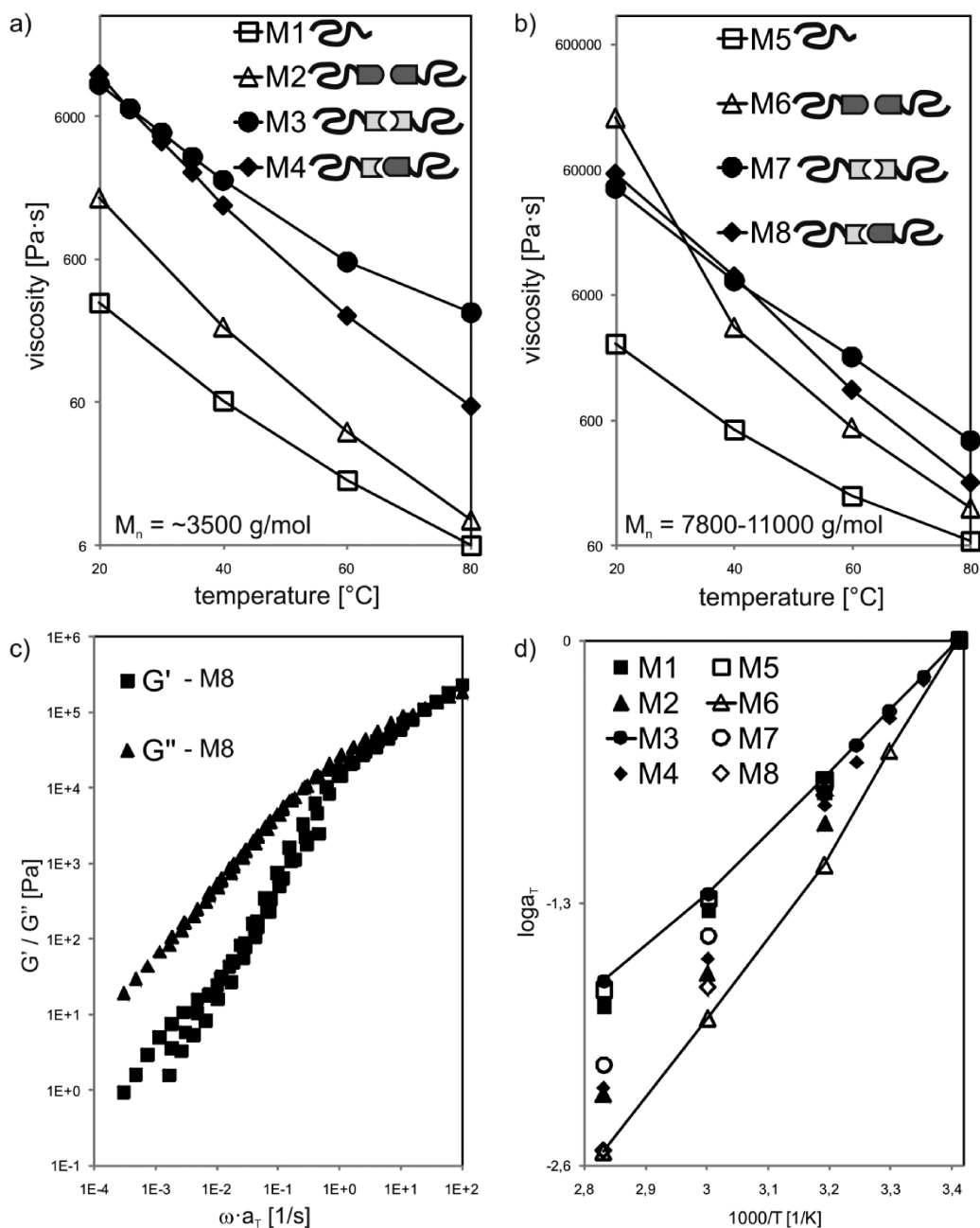


**Figure 4.** Viscosity vs temperature for (a) monofunctional PIBs (M1–M4) with a molecular weight of  $\sim 3500$  g/mol and (b) monofunctional PIBs (M5–M8) with a molecular weight of  $\sim 10000$  g/mol, (c) master curve of the storage and loss modulus for M8, and (d) temperature dependency of the horizontal shift factor  $a_T$  for M1–M8. The two lines mark the extremes in the temperature dependence.

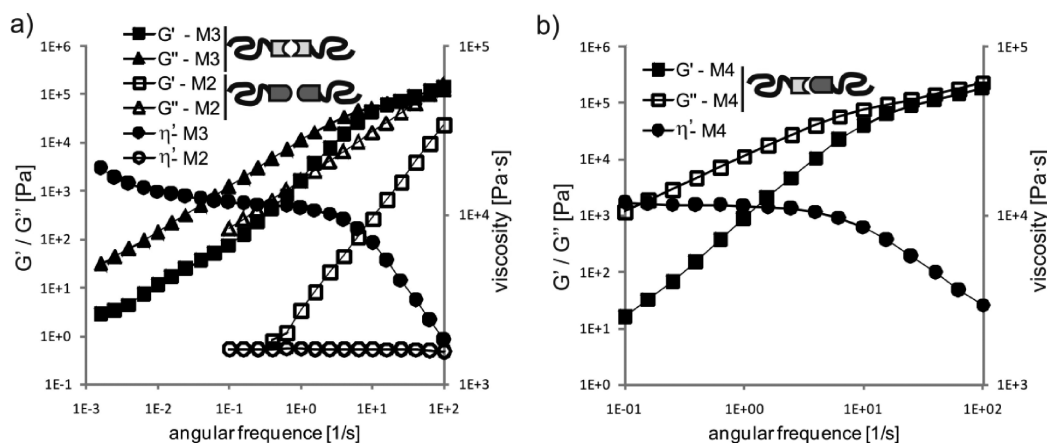
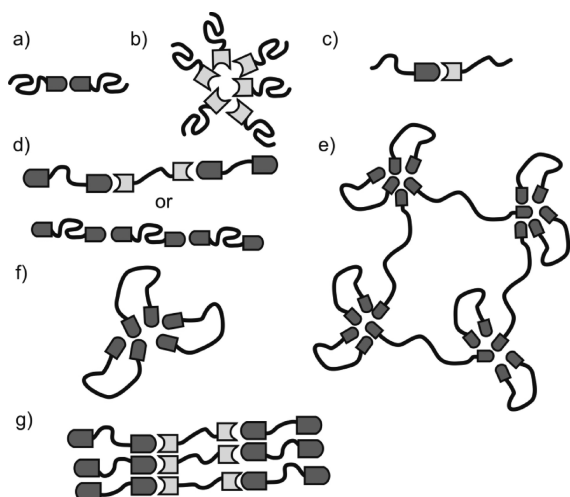


**Figure 5.** Viscosity (real part of the viscosity), storage ( $G'$ ), and loss modulus ( $G''$ ) vs angular frequency at 20 °C (a) for M3 and M2 and (b) for M4.



**Scheme 3. Possible Structures Formed by Aggregation via Hydrogen Bonds of Monofunctional (a–c) and Bifunctional Polymers (d–g)**



an exchange of their counterparts on the same time scale as the external mechanical perturbation and hence the viscosity additionally decreases. This proves the specific aggregation of the polymers via the hydrogen-bonding moieties used as shown in Scheme 3c.

For the monofunctional samples **M5**–**M8** with a molecular weight of  $\sim 10\,000\text{ g mol}^{-1}$  the melt viscosity in dependence on temperature is displayed in Figure 4b. In comparison to the lower molecular weight analogues (**M1**–**M4**) the values for the melt viscosity are about 1 order of magnitude larger, suggesting an entangled melt. This is somewhat surprising as the critical molecular weight for entanglement ( $M_c$ ) was reported to be  $16\,020$  or  $17\,000\text{ g mol}^{-1}$  for poly(isobutylene).<sup>43,44</sup> Despite their higher viscosities, the curves for **M5**, **M7**, and **M8** reveal a similar shape in comparison to their lower molecular weight analogues. The increased melt viscosity values for **M7** and **M8** indicate cluster formation (**M7**) as well as a supramolecular A–B-type aggregation (**M8**).

A significant difference is observed for pure thymine-functionalized PIB (**M6**) at  $20\text{ }^\circ\text{C}$ , where the highest viscosity within this series is observed. In this sample, the huge drop of the viscosity by increasing the temperature to  $40\text{ }^\circ\text{C}$  indicates the presence of only weak interactions between thymine–thymine groups. Since the molecular weight of the thymine-functionalized PIB in **M6** is  $\sim 11\,000\text{ g/mol}$ , the interaction of the polymer chains between spatial separate supramolecular aggregates can be seen as a possible cause for the unexpected high values for the melt viscosity at  $20\text{ }^\circ\text{C}$ . The fact that for **M6** a zero shear viscosity was not observed within our frequency range confirms this assumption. By increasing the temperature and thus increasing the chain mobility, such an interaction is no longer possible and a huge drop of the melt viscosity is observed.

Although the supramolecular interaction introduced by the attachment of hydrogen-bonding moieties onto the PIB chain is strongly temperature dependent, master curves for the monofunctional samples **M1**–**M8** could be generated by using simple horizontal frequency–temperature superposition. This was possible since the shape of the storage and loss modulus vs angular frequency curves remained similar with increasing temperature.<sup>48</sup> As an example, the master curve of **M8** is displayed in Figure 4c as well as the shift factors for **M1**–**M8** in Figure 4d. Figure 4d reveals a stronger temperature dependence of the shift factors for the samples containing a hydrogen-bonding moiety (dynamic interactions) in comparison to the nonfunctionalized samples **M1** and **M5**.

Only **M3** shows a temperature dependence similar to those of the nonfunctionalized PIBs, which can be assigned to the formation of nondynamic clusters, which were stable up to temperatures of  $90\text{ }^\circ\text{C}$  (as revealed by SAXS measurement) and thus covering the whole temperature range of the rheology experiment.

**SAXS Measurements of Monofunctional Polymers.** In order to check for structural signs of the self-aggregation of samples with solely pendant thymine and 2,6-triazine moieties, samples **M2**–**M4** were investigated by SAXS measurements. While for pure thymine-functionalized PIB **M2** no excess scattering could be observed (possibly due to a lack of contrast, see Supporting Information), SAXS measurements for **M3** and **M4** in Figure 6 clearly show temperature-dependent excess peaks. For pure 2,6-diaminotriazine-functionalized PIB **M3** the ratio between the positions of the observed scattering peaks is  $1:\sqrt{2}:\sqrt{3}$ , which can be assigned to a BCC lattice (body-centered cubic). A BCC grid is typical for block copolymers made of a long and a short block.<sup>49</sup> Since the 2,6-diaminotriazine-functionalized PIB **6a** (**M3**) can be seen as a block copolymer where one block is the PIB chain and the other one is the 2,6-diaminotriazine moiety, this observation is in agreement with the structure of the polymer. It is noteworthy that the BCC structure is destroyed only at temperatures above  $90\text{ }^\circ\text{C}$ , thus explaining the high values for the melt viscosity up to temperatures of  $80\text{ }^\circ\text{C}$  and the lack of terminal flow. The BCC structure is formed again after cooling to  $20\text{ }^\circ\text{C}$ , indicating a reversible cluster formation. The observed periodicity of the BCC structure  $d = 2\pi/q_{\text{max}} \sim 6.5\text{ nm}$  compares reasonably well with the estimated end-to-end distance of the PIB chains ( $2\text{ nm}$  as calculated with the ideal chain model), taking into account that the chains might in reality be considerably stretched.

For the equimolar mixture **M4** of thymine- and 2,6-diaminotriazine-functionalized PIB the SAXS measurement reveals excess scattering, but no well-ordered structure. The presence of thymine groups in **M4** suppresses the formation of a BCC structure of the 2,6-diaminotriazine-functionalized PIB chains and can thus be seen as an additional indication for a selective thymine–2,6-diaminotriazine interaction in the solid state.

For the monofunctional analogues with a higher molecular weight (**M6**–**M8**) SAXS measurements were performed in order to prove whether there is an influence of the molecular weight on the structure formation. For pure thymine-functionalized PIB **M6** again only a very weak excess scattering signal could be observed (see Supporting Information). In contrast to **M3** (Figure 6b), the higher molecular weight analogue **M7** shows no well-ordered periodic structure (Figure 6d). The equimolar mixture **M8** of monofunctional thymine- and 2,6-diaminotriazine-functionalized PIB chains reveals (Figure 6c) again a peak, but in comparison to the low molecular weight analogue sample **M4** (Figure 6a) at lower  $q$ . This difference reflects the higher molecular weight of **M8**. The different results in SAXS measurements for samples **M6**–**M8** again are compatible with a selective thymine–2,6-diaminotriazine interaction in the solid state.

**Association of Bifunctional Polymers Studied by Melt Rheology.** In addition to the monofunctional samples, the respective bifunctional PIB samples with a molecular weight of  $\sim 3500\text{ g/mol}$  were investigated by dynamic rheology. In these samples the formation of more complex supramolecular assemblies is possible. For bifunctional thymine-functionalized PIB **M10** or bifunctional 2,6-diaminotriazine-functionalized PIB **M11** the formation of a large variety of more complex aggregates, such as supramolecular chains or cross-linked clusters can be expected (Scheme 3d–f). The presence of both



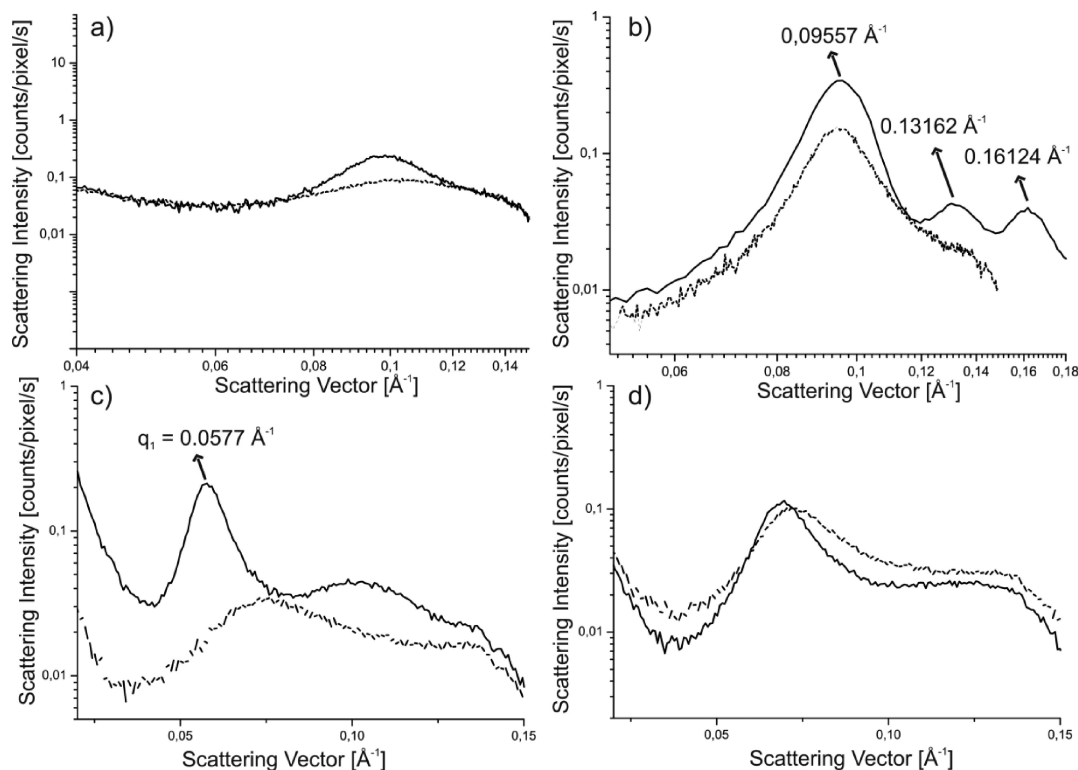


**Figure 6.** SAXS measurements for (a) **M4** at 20 °C (solid line) and 120 °C (dashed line), (b) **M3** at 20 °C (solid line) and 120 °C (dashed line), (c) **M8** at 20 °C (solid line) and 120 °C (dashed line), and (d) **M7** at 20 °C (solid line) and 120 °C (dashed line).

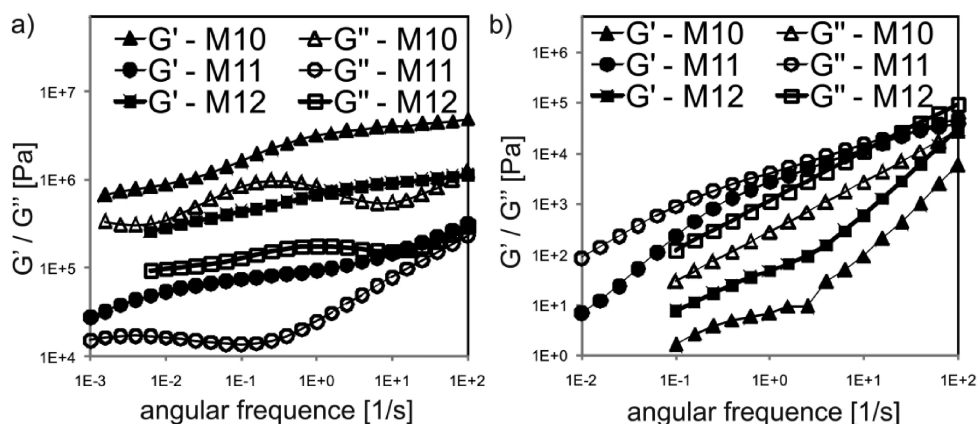


**Figure 7.** Frequency dependence of storage and loss modulus for **M10–M12** at (a) 20 and (b) 80 °C.

bis-thymine- and bis-2,6-diaminotriazine-functionalized PIB chains in **M12** should lead to a preferred formation of supramolecular  $(-A-B-)_n$  chains, possibly accompanied by aggregation of those chain-end connections (Scheme 3g).

Pure allyl-functionalized PIB **M9** reveals similar values for the melt viscosity in comparison to the monofunctional analogue **M1** with a similar molecular weight, since the presence of a second allyl end group does not lead to a significant change in the melt viscosity (see Table 2).

In the case of **M10**, **M11**, and **M12** the presence of bifunctional polymer chains leads to a rubberlike material which is not flowing at 20 and 40 °C, while in the case of **M11** even at 60 °C no flowing was observed (see Supporting Information). Surprisingly, pure bis-thymine-functionalized PIB **M10** exhibits higher values for the storage modulus (Figure 7a) than **M12**, although a stronger interaction is expected for the bis(2,6-diaminopyridine) sample. For bis-2,6-diaminotriazine-functionalized **M11** the smallest values for the storage modulus were observed,

although the monofunctional analogue **M3** revealed the strongest effect on storage modulus within the series **M1–M4** due to the formation of strong clusters. At 60 °C **M10** and **M12** flow but with large differences in the values for the melt viscosity. While for pure thymine-functionalized PIB **M10** a value of 2370 Pa·s was observed at 60 °C, the equimolar mixture of thymine- and 2,6-diaminotriazine-functionalized PIB chains **M12** reveals a value of 25 000 Pa·s. This observation leads to the assumption that the supramolecular aggregates in **M10** and **M12** differ from each other. As already mentioned, the undirected supramolecular interaction between two or more thymine groups (or 2,6-diaminotriazine groups) can lead to a network as displayed in Scheme 3e, while the more directed interaction between thymine and 2,6-diaminotriazine groups in **M12** leads preferred to the formation of long supramolecular  $(-A-B-)_n$  chains. The higher values for **M10** for the storage modulus at 20 and 40 °C can thus be explained by the higher rigidity of the supramolecular network in comparison to the extended, sheetlike

supramolecular aggregates shown in Scheme 3g. By increasing the temperature ( $> 60\text{ }^{\circ}\text{C}$ ), the weak thymine–thymine interaction is released to a higher extent than the stronger thymine–2,6-diaminotriazine interaction, thus explaining the significantly lower viscosities of **M10** in comparison to **M12** at  $60\text{ }^{\circ}\text{C}$ .

For linear high molecular weight PIB the plateau modulus was reported to be in the range of  $2.5 \times 10^5$ – $3.2 \times 10^5\text{ Pa}$ .<sup>43,50</sup> In comparison, samples **M10** ( $\sim 1 \times 10^7\text{ Pa}$ ) and **M12** ( $\sim 1 \times 10^6\text{ Pa}$ ) reveal much higher values for the plateau modulus. This observation can be explained by the formation of supramolecular cross-links as a result of undirected interactions like those displayed in Scheme 3e. These undirected interactions are especially existent in **M10**, since here only thymine groups are present.

**M12** reveals a lower plateau value than **M10**, since the undirected interactions are suppressed by the strong and directed thymine–2,6-diaminotriazine interaction, and thus the amount of supramolecular cross-links is reduced. The fact that the plateau modulus for **M12** is still higher than the reported plateau value for the linear PIB may indicate that also for **M12** additional supramolecular cross-links between different end group aggregates are present. However, the network formation of **M10** was not observed for the bis(2,6-diaminotriazine)-telechelic PIB **M11** to the same extent. Until now, it cannot be specified why **M11** reveals the smallest values for the storage modulus within this series as the formation of clusters (like in **M3**) should lead to the formation of a strongly cross-linked network as displayed in Scheme 3e. A possible explanation would be the partial formation of aggregates like in Scheme 3f, which would lead to a nonbridged cross-linked structure. The fact that **M11** does not flow at  $60\text{ }^{\circ}\text{C}$  and reveals at  $80\text{ }^{\circ}\text{C}$  with  $8450\text{ Pa}\cdot\text{s}$  a much higher viscosity than **M10** ( $292\text{ Pa}\cdot\text{s}$ ) and **M12** ( $1210\text{ Pa}\cdot\text{s}$ ) indicates that the formation of strong clusters are also present up to high temperatures in **M11**.

**SAXS Measurements of Bifunctional Polymers.** For polymeric samples containing bifunctional PIBs **M10**–**M12** SAXS measurements do not reveal any ordered structure (see Supporting Information). According to the monofunctional samples **M2** and **M6** for bis-thymine-functionalized **M10** no excess scattering was observed. Although low molecular weight 2,6-diaminotriazine-functionalized PIB **M3** reveals a BCC structure, for the bifunctionalized analogous **M11** no ordered structure was observed, which can be assigned to the reduced mobility of the polymer chain if one end is already attached to some kind of aggregate.

## Conclusion

Supramolecular polymers bearing mono- and bifunctional chain ends with hydrogen-bonding units were prepared, and their association behavior was investigated by dynamic rheology in the melt state and SAXS. The synthetic approach combined living cationic polymerization with either azide/alkyne “click” reactions or nucleophilic substitution reactions and enabled a full end-group transformation to the final polymers, modified with either thymine- or 2,6-diaminotriazine end groups.

Subsequent rheological measurements were conducted on either pure mono- or bifunctionalized polymers or of equimolar mixtures generating A/B-type aggregates. It could be demonstrated that supramolecular polymers and their mixtures show a strong and reversible temperature dependence of their mechanical behavior. The temperature dependence of the rheological properties is stronger than for the nonfunctionalized PIB homopolymers. This clearly demonstrates the additional effect of the dynamics of the hydrogen bonds compared to solely chain dynamics. Generally, the effects as e.g. the increase in viscosity is not compatible with a simple specific connection of two

polymers by a single hydrogen bond. Obviously, larger aggregates of chains are formed due to less specific interactions. The formation of more complex aggregates such as microphase-separated cluster-type assemblies is in some cases even reflected by the appearance of regular peaks in the small-angle scattering pattern. Nevertheless, the specific aggregation between thymine or 2,6-diaminotriazine end groups clearly showed up in the rheological properties. Therefore, not only the strength of the individual hydrogen bond but also secondary effects such as unspecific clustering of the H-bonds have to be taken into account in order to achieve further understanding and control of supramolecular polymers in the melt state.

**Acknowledgment.** We are thankful for grants DFG BI 1337/7-1 (F.H., W.H.B.) and DFG TH 1281/5-1 as well as grants DFG INST 271/249-1, INST 271/247-1, and INST 271/248-1 (W.H.B.) for financial support. Significant investments into our NMR infrastructure from the European Regional Development Fund (ERDF) by the European Union are gratefully acknowledged. J.B. and S.G. acknowledge support by ProNet-T3 (BMBF).

**Supporting Information Available:** Detailed information (synthesis, column chromatography, NMR data) for compound **9** as well as thymine-functionalized PIBs **4**, **5** and 2,6-diaminotriazine-functionalized PIBs **6a**–**c**, **7**; MALDI-TOF-MS spectra for thymine-functionalized PIB **5** and 2,6-diaminotriazine-functionalized PIB **7**; SAXS measurements of **M2**, **M6**, **M10**, **M11**, **M12**; temperature-dependent SAXS measurement for **M3**; detailed description of the NMR titration experiments, rheology data for **M10**, **M11**, and **M12** at  $40$  and  $60\text{ }^{\circ}\text{C}$ ; glass transition temperatures for **M1**–**M12** measured via DSC. This material is available free of charge via the Internet at <http://pubs.acs.org>.

## References and Notes

- (1) Binder, W. H.; Zirbs, R. In *Advances Polymer Science*; Binder, W., Ed.; Springer: Berlin, 2007; Vol. 207, pp 1–78.
- (2) Bouteiller, L. In *Advances Polymer Science*; Binder, W. H., Ed.; Springer: Berlin, 2007; Vol. 207, pp 79–112.
- (3) Brunsveld, L.; Folmer, B. J. B.; Meijer, E. W.; Sijbesma, R. P. *Chem. Rev.* **2001**, *101*, 4071–4098.
- (4) ten Brinke, G.; Ruokolainen, J.; Ikkala, O. In *Advances Polymer Science*; Binder, W. H., Ed.; Springer: Berlin, 2007; Vol. 207, pp 113–177.
- (5) Xu, H.; Srivastava, S.; Rotello, V. In *Advances Polymer Science*; Binder, W. H., Ed.; Springer: Berlin, 2007; Vol. 207, pp 179–198.
- (6) Cordier, P.; Tournilhac, F.; Soulié-Ziakovic, C.; Leibler, L. *Nature* **2008**, *451*, 977–980.
- (7) Montarnal, D.; Cordier, P.; Soulié-Ziakovic, C.; Tournilhac, F.; Leibler, L. *J. Polym. Sci., Part A: Polym. Chem.* **2008**, *46*, 7925–7936.
- (8) Kautz, H.; van Beek, D. J. M.; Sijbesma, R. P.; Meijer, E. W. *Macromolecules* **2006**, *39*, 4265–4267.
- (9) Wisse, E.; Spiering, A. J. H.; Pfeifer, F.; Portale, G.; Siesler, H. W.; Meijer, E. W. *Macromolecules* **2009**, *42*, 524–530.
- (10) Dankers, P. Y. W.; Harmsen, M. C.; Brouwer, L. A.; Van Luyn, M. J. A.; Meijer, E. W. *Nature Mater.* **2005**, *4*, 568–574.
- (11) Binder, W. H.; Petraru, L.; Roth, T.; Groh, P. W.; Pálfi, V.; Keki, S.; Ivan, B. *Adv. Funct. Mater.* **2007**, *17*, 1317–1326.
- (12) Hackethal, K.; Döhler, D.; Tanner, S.; Binder, W. H. *Macromolecules* **2010**, *43*, 1761–1770.
- (13) Binder, W. H.; Bernstorff, S.; Kluger, C.; Petraru, L.; Kunz, M. *Adv. Mater.* **2005**, *17*, 2824–2828.
- (14) Kunz, M. J.; Hayn, G.; Saf, R.; Binder, W. H. *J. Polym. Sci., Part A: Polym. Chem.* **2004**, *42*, 661–674.
- (15) Cates, M. E. *Macromolecules* **1987**, *20*, 2289–2296.
- (16) Hammes, G. G.; Park, A. C. *J. Am. Chem. Soc.* **1968**, *90*, 4151–4157.
- (17) Sontjens, S. H. M.; Sijbesma, R. P.; van Genderen, M. H. P.; Meijer, E. W. *J. Am. Chem. Soc.* **2000**, *122*, 7487–7493.
- (18) Embrechts, A.; Schönherr, H.; Vancso, G. J. *J. Phys. Chem. B* **2008**, *112*, 7359–7362.
- (19) Vancso, G. *Angew. Chem., Int. Ed.* **2007**, *46*, 3794–3796.

- (20) Zou, S.; Schönherr, H.; Vancso, G. J. *Angew. Chem., Int. Ed.* **2005**, *44*, 956–959.
- (21) Knoben, W.; Besseling, N. A. M.; Bouteiller, L.; Cohen-Stuart, M. A. *Phys. Chem. Chem. Phys.* **2005**, *7*, 2390–2398.
- (22) Knoben, W.; Besseling, N. A. M.; Cohen-Stuart, M. A. *J. Chem. Phys.* **2007**, *126*, 024907–9.
- (23) Courtois, J.; Baroudi, I.; Nouvel, N.; Degrandi, E.; Pensec, S.; Ducouret, G.; Chanéac, C.; Bouteiller, L.; Creton, C. *Adv. Funct. Mater.* **2010**, *20*, 1803–1811.
- (24) Pensec, S.; Nouvel, N.; Guilleman, A.; Creton, C.; Boué, F. o.; Bouteiller, L. *Macromolecules* **2010**, *43*, 2529–2534.
- (25) Müller, M.; Dardin, A.; Seidel, U.; Balsamo, V.; Ivan, B.; Spiess, H. W.; Stadler, R. *Macromolecules* **1996**, *29*, 2577–2583.
- (26) Schirle, M.; Hoffmann, I.; Pieper, T.; Kilian, H.-G.; Stadler, R. *Polym. Bull.* **1996**, *36*, 95–102.
- (27) Loveless, D. M.; Abu-Lail, N. I.; Kaholek, M.; Zauscher, S.; Craig, S. L. *Angew. Chem., Int. Ed.* **2006**, *45*, 7812–7814.
- (28) Serpe, M. J.; Craig, S. L. *Langmuir* **2007**, *23*, 1626–1634.
- (29) Yount, W. C.; Loveless, D. M.; Craig, S. L. *J. Am. Chem. Soc.* **2005**, *127*, 14488–14496.
- (30) Yount, W. C.; Loveless, D. M.; Craig, S. L. *Angew. Chem., Int. Ed.* **2005**, *44*, 2746–2748.
- (31) Sivakova, S.; Bohnsack, D. A.; Mackay, M. E.; Suwanmala, P.; Rowan, S. J. *J. Am. Chem. Soc.* **2005**, *127*, 18202–18211.
- (32) Langille, N. F.; Jamison, T. F. *Org. Lett.* **2006**, *8*, 3761–3764.
- (33) Lindsell, E. W.; Murray, C.; Preston, P. N.; Woodman, T. A. J. *Tetrahedron* **2000**, *56*, 1233–1245.
- (34) Binder, W. H.; Kunz, M. J.; Kluger, C.; Hayn, G.; Saf, R. *Macromolecules* **2004**, *37*, 1749–1759.
- (35) Ammann, C.; Meier, P.; Merbach, A. J. *Magn. Reson.* **1982**, *46*, 319–321.
- (36) Kennedy, J. P.; Iván, B. *Designed Polymers by CARBOCATIONIC MACROMOLECULAR ENGINEERING - Theory and Practice*; Carl Hanser Verlag: Munich, 1992.
- (37) Binder, W. H.; Enders, C.; Herbst, F.; Hackethal, K. Synthesis and Self Assembly of Hydrogen-Bonded Supramolecular Polymers. In *Complex Macromolecular Architectures: Synthesis, Characterization, and Self Assembly*; Hadjichristidis, N.; Tezuka, Y.; Hirao, A., Eds.; Wiley-VCH: Berlin, 2010, in press.
- (38) Binder, W. H.; Kluger, C. *Curr. Org. Chem.* **2006**, *10*, 1791–1815.
- (39) Binder, W. H.; Sachsenhofer, R. *Macromol. Rapid Commun.* **2007**, *28*, 15–54.
- (40) Binder, W. H.; Sachsenhofer, R. *Macromol. Rapid Commun.* **2008**, *29*, 952–981.
- (41) Binder, W. H.; Zirbs, R. “Click” Chemistry in Macromolecular Synthesis; John Wiley & Sons, Inc.: New York, 2002.
- (42) Beijer, F. H.; Sijbesma, R. P.; Vekemans, J. A. J. M.; Meijer, E. W.; Kooijman, H.; Spek, A. L. *J. Org. Chem.* **1996**, *61*, 6371–6380.
- (43) Aharoni, S. M. *Macromolecules* **1986**, *19*, 426–434.
- (44) Fox, T. G.; Flory, P. J. *J. Phys. Chem.* **1951**, *55*, 221–234.
- (45) Gong, H.; Krische, M. J. *J. Am. Chem. Soc.* **2005**, *127*, 1719–1725.
- (46) Dardin, A.; Boeffel, C.; Spiess, H. W.; Stadler, R.; Samulski, E. T. *Acta Polym.* **1995**, *46*, 291–299.
- (47) Wisse, E.; Govaert, L. E.; Meijer, H. E. H.; Meijer, E. W. *Macromolecules* **2006**, *39*, 7425–7432.
- (48) van Beek, D. J. M.; Spiering, A. J. H.; Peters, G. W. M.; te Nijenhuis, K.; Sijbesma, R. P. *Macromolecules* **2007**, *40*, 8464–8475.
- (49) Hamley, I. W. *The Physics of Block Copolymers*; Oxford University Press: Oxford, 1998.
- (50) Fetters, L. J.; Lohse, D. J.; Richter, D.; Witten, T. A.; Zirkel, A. *Macromolecules* **1994**, *27*, 4639–4647.